metals

MDPI

Review

Progress in Melting-Flow Characteristics of Titanium-Bearing Blast Furnace Slag

Guang Li [2], Shuai Wang [1,2,*], Yufeng Guo [1,2,*], Mao Chen [1,3], Yihan Huang [2], Feng Chen [1,2], Jinlai Zhang [2] and Lingzhi Yang [2]

[1] State Key Laboratory of Vanadium and Titanium Resources Comprehensive Utilization, Panzhihua 617000, China; mao.chen@uqconnect.edu.au (M.C.)
[2] School of Minerals Processing and Bioengineering, Central South University, Changsha 410083, China
[3] Pangang Group Research Institute Co., Ltd., Panzhihua 617000, China
* Correspondence: wang_shuai@csu.edu.cn (S.W.); yfguo@csu.edu.cn (Y.G.); Tel.: +86-0731-88830346 (Y.G.)

Abstract

Vanadium–titanium magnetite is a critical strategic polymetallic mineral resource in China, and blast furnace smelting represents the dominant large-scale industrial process for its utilization. The melting and fluidity properties of titanium-bearing blast furnace slags (TBFS) directly govern stable blast furnace operation and the recovery efficiency of vanadium–titanium resources. This paper systematically reviews research progress on the melting and flow characteristics of TBFS. The influences of main components (TiO_2, CaO/SiO_2, MgO, Al_2O_3), trace oxides, and strongly reduced products TiC and TiN on slag mineral phases, break point temperature (T_{Br}) and viscosity are summarized. Combined with X-ray diffraction (XRD), Fourier transform infrared spectroscopy (FTIR), Raman characterizations and FactSage thermodynamic calculations, the inherent mechanisms are revealed from the perspectives of microstructural network polymerization and crystalline phase precipitation. TiO_2 exerts dual effects: it depolymerizes the silicate network to reduce slag viscosity while promoting the precipitation of high-melting-point perovskite. Al_2O_3 intensifies network polymerization and impairs slag fluidity. MgO, basicity, MnO and BaO can decrease slag viscosity. Solid particles of TiC and TiN generated under the strong reducing atmosphere inside blast furnaces drastically increase slag viscosity and Tbr. This paper proposes that future research should focus on slag systems with higher TiO_2 contents, so as to provide theoretical support for the high-efficiency blast furnace smelting of VTM and resource utilization of titanium-bearing slags.

Keywords: viscosity; slag structure; perovskite; blast furnace slag

Check for updates

Academic Editors: Elmira Moosavi-Khoonsari and Mohammad Jahazi

Received: 29 May 2026
Revised: 23 June 2026
Accepted: 24 June 2026
Published: 27 June 2026

Copyright: © 2026 by the authors. Licensee MDPI, Basel, Switzerland. This article is an open access article distributed under the terms and conditions of the Creative Commons Attribution (CC BY) license.

1. Introduction

As a key polymetallic ore containing iron, vanadium and titanium, vanadium–titanium magnetite (VTM) is strategically vital for global iron and titanium industries. Major ore reserves are concentrated in China, Russia, South Africa and Australia [1]. The proven reserves in China amount to 9.83 billion tonnes, and the inferred reserves are in excess of 30 billion tonnes [2]. Within China, VTM deposits are mainly distributed in the Panxi region of Sichuan, Chengde of Hebei and Shanxi Province. Resource exploitation in these areas has become an important support for the iron–steel and titanium industries [3]. However, its complex chemical composition and unique mineral structure have long restricted the comprehensive utilization efficiency of VTM. In particular, there remain numerous

challenges in achieving high-efficiency recovery under economic and environmentally friendly conditions [4]. Accordingly, in-depth research on resource characteristics and comprehensive utilization technologies of VTM is of great significance for ensuring the sustainable supply of strategic metal resources in China.

Figure 1 illustrates the mainstream utilization routes of VTM. After ore beneficiation, most titanium in raw ores is enriched in vanadium–titanium magnetite concentrate, while the residual titanium remains in iron beneficiation tailings [5]. Two primary technical routes are currently adopted for concentrate processing: blast furnace smelting and non-blast furnace processes. The blast furnace route features mature techniques and large throughput, and has been widely applied in China and Russia. Among non-blast furnace routes, only the pre-reduction electric furnace process has achieved industrial application in South Africa and New Zealand [6]. During blast furnace smelting, iron and vanadium are reduced and transferred into hot metal, the majority of titanium migrates into slags to form titanium-bearing blast furnace slags (TBFS) [3]. TBFS is classified by TiO_2 content into low-titanium (<10 wt%), medium-titanium (10–20 wt%) and high-titanium slag (>20 wt%) [7]. It is also categorized by Al_2O_3 into four grades: low-aluminum (<14 wt%), medium-aluminum (14–16 wt%), high-aluminum (16–18 wt%) and ultra-high-aluminum slag (>18 wt%) [8].

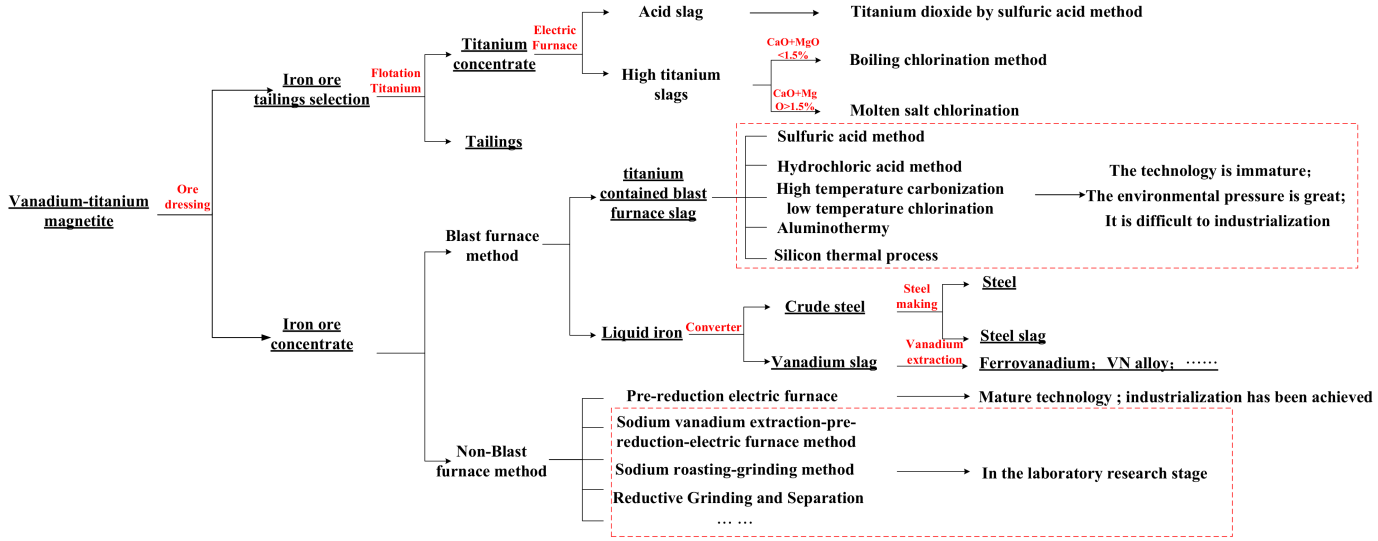


Figure 1. Utilization approaches of VTM.

Table 1 presents chemical compositions of TBBS from Chengde and Panzhihua Iron and Steel. Their TiO_2 contents are 12.26 wt% and 23 wt% respectively, confirming prominent titanium enrichment in blast furnace slag. Long-term stockpiling of high-titanium slag wastes land resources, impairs soil ecology and causes titanium resource loss [9]. Low titanium grade and difficult phase separation limit the economic benefits of TBBS utilization, while elevated slag TiO_2 worsens blast furnace stability. Thus, slag system optimization and matched comprehensive utilization technologies are essential for efficient titanium recovery. Most TBBS utilization technologies remain laboratory-scale at present. The only operational demonstration line developed by Panzhihua Iron and Steel adopts high-temperature carbonization coupled with low-temperature chlorination, with an annual treatment capacity of 100,000 t TBBS and a 37,000 t $TiCl_4$ output [10,11].

Table 1. Composition of TBFS.

Composition	Chemical Composition/wt%								R2
	CaO	MgO	SiO_2	Al_2O_3	TiO_2	V_2O_5	TiC + TiN	S	
Chengde Steel (Adapted from [12])	31.37	11.66	28.23	13.42	12.26	0.2	0.63	0.78	1.19
Panzhihua Steel	28.37	8.63	26.21	14.63	22.87	0.25	1.28	0.48	1.08

Within blast furnace smelting, slag physicochemical properties dominate furnace operation stability and slag–iron separation performance, among which melting and flow behaviors act as the most critical indicators. Distinct from conventional iron ore smelting, vanadium–titanium magnetite contains abundant TiO_2. As a multivalent element, titanium is reduced to low-valence titanium species under the strongly reducing atmosphere inside blast furnaces, and further generates high-melting solid phases including TiC and TiN. These solid particles remarkably raise the Tbr and viscosity of slag, severely disrupting normal smelting [12]. To raise the enrichment level of TiO_2 in blast furnace slag and boost the recovery efficiency of titanium resources, it is necessary to simultaneously tackle practical production problems such as elevated slag viscosity and deteriorated fluidity induced by high-titanium components. Current regulation strategies mainly fall into two categories: adjusting blast furnace smelting temperature and internal atmosphere and optimizing the chemical composition of slag. At present, the operating temperature and reducing atmosphere parameters of domestic vanadium–titanium blast furnaces have been relatively fixed, leaving little room for drastic adjustment of operation regimes. Accordingly, slag system optimization via component regulation has become a more feasible and dominant technical route.

TBFS mainly consists of TiO_2, CaO, SiO_2, Al_2O_3 and MgO. Variations in the proportions of these components directly affect the precipitation behavior of mineral phases at high temperatures, thereby drastically altering critical physicochemical properties of TBFS including melting and flow characteristics. Distinct disparities exist in the contents of trace metallic elements such as V, Mn and Cr among titanium slags produced from vanadium–titanium magnetite ores of different mining areas. The regulatory effect of trace components on the viscous flow performance of slag has gradually become a research hotspot in this field. Precisely adjusting the mass ratios of major components can improve the melting and flow behaviors of molten slag, reduce viscosity and T_{Br}, and consequently guarantee stable blast furnace operation while increasing titanium content in slag [13–16].

Accordingly, this paper systematically reviews the research progress on melting and flow characteristics of TBFS, and explores corresponding performance optimization strategies, so as to provide critical references for promoting the technological development of the comprehensive utilization of VTM.

The literature retrieval databases used in this paper include Web of Science, MDPI, CNKI and Wanfang Data, with the retrieval year set from 1930 to 2026. Chinese and English keywords center on TBFS, flow characteristics, viscosity, perovskite, Ti(C,N) and other relevant terms. After retrieval, duplicate documents are removed via software and manual screening. Subsequently, two authors independently conduct primary screening based on titles and abstracts, eliminating studies with irrelevant themes, pure review papers and conference abstracts. The full texts of the remaining studies are read thoroughly for secondary screening in accordance with established inclusion and exclusion criteria. Only original papers containing complete quantitative physical property data, microscopic characterization results or thermodynamic experimental data are retained, while duplicate studies, those with missing data and studies merely focusing on the utilization of slag as

building materials are excluded. Finally, qualified studies are classified and filed into three major categories: melting behavior, flow behavior and influence mechanism, and their experimental data are uniformly extracted for comparative analysis.

2. Research Progress on Melting and Flow Characteristics of TBFS

This subsection systematically sorts out existing studies on slag system regulation of TBFS and clarifies the evolution laws of slag melting and fluidity under various component conditions as well as their internal influencing mechanisms. Meanwhile, experimental conclusions from different studies are compared and analyzed to provide theoretical references for slag system optimization and regulation in blast furnace smelting of vanadium–titanium magnetite.

2.1. Characteristics

Slag melting characteristics denote comprehensive thermal behaviors during heating melting, covering softening property, melting temperature range, characteristic melting temperature and phase transformation. Phase transformation and Tbr variation are core factors governing slag fluidity, and critically determine slag–iron separation in furnace hearth. Phase transformation modifies slag internal network structure and its melting characteristics. Fluidity declines drastically below Tbr and impedes slag–iron separation. This section reviews current research to support practical blast furnace smelting regulation.

2.1.1. Mineral Composition and Phase Transformation

The phase types in TBFS derived from VTM are relatively stable, mainly including perovskite ($CaTiO_3$), pyroxene group minerals ($Ca(Mg,Fe,Al)(Si,Al)_2O_6$), magnesium–aluminum spinel ($MgAl_2O_4$) and melilite group minerals ($Ca_2(Mg,Fe)Si_2O_7$) [5,17–19]. Figure 2 presents the microstructural morphology of blast furnace slag obtained from vanadium–titanium magnetite smelting at Panzhihua Iron and Steel Group. Point A in the figure corresponds to perovskite, which is the primary titanium-bearing mineral in TBFS. Ions such as Ca^{2+} and Mg^{2+} in pyroxene phases can be partially substituted by Ti^{4+} to form titanium-containing pyroxene. Depending on TiO_2 content, these pyroxenes can be subdivided into Panzhihua-titanium diopside (Point B) and titanium-rich diopside (Point C), which are major Ti-enriched phases. Point D denotes metallic iron, while Point E represents amorphous TiC generated during the reduction process [20].

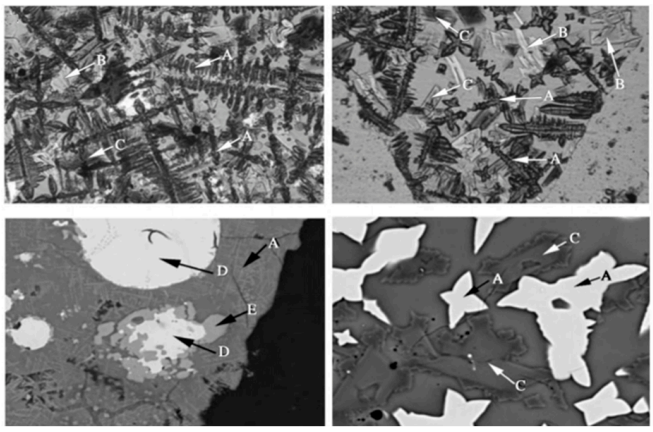


Figure 2. Microstructural morphology of TBFS from a certain steel plant. The figure represent different regions of one sample and are intended to illustrate the types of phases present in the sample. (A) perovskite. (B) Clinochlore Diopside. (C) Titanium-rich diopside. (D) metallic iron. (E) TiC. (Reprinted with permission from Ref. [20]. 2017, Metallurgical Analysis).

Mineral phase transformation is a common phenomenon in high-temperature smelting processes. When external conditions such as slag temperature and composition change, the crystal structure or chemical composition of slag phases will be modified. During smelting, phase transformation acts as a critical factor affecting the melting and flow characteristics of slag. Table 2 lists the differences in melting point of the main phases in TBFS. It can be seen from the table that perovskite, magnesium–aluminum spinel and titanium carbonitride have high melting point, while other phases have relatively low melting points.

Table 2. Comparison of physicochemical properties of different mineral phases.

Specific Mineral Phase	Melting Point (°C)
Perovskite	1970–2100
Ti-rich Diopside	1380–1450
Panzhihua-titanium Diopside	1420–1480
Anorthite	1550–1580
Augite/Diopside	1390–1460
Mg-Al Spinel	2135–2150
Titanium Carbonitride	2950–3150
Glassy Phase	No fixed melting point (softening range: 800–1200)

During the phase transformation of slag, the precipitation of high-melting-phase constituents adversely impairs slag fluidity. Therefore, the investigation of phase transformation is essential for slag system regulation. Studies have shown that under strong reducing conditions, bead-like perovskite in TBFS transforms into dispersed titanium carbide, accompanied by the disappearance of dark green tabular titanium-rich diopside. A higher titanium dioxide content favors the transformation of slag phases toward titanium-containing phases such as perovskite and titanium carbonitride [20–23]. Increasing alumina content elevates the initial precipitation temperature and precipitation capacity of gehlenite (low-melting-point phase) [16,24–26]. Deng et al. [25] reported that with the rising magnesium oxide content, the mass fraction of perovskite in slag decreases initially and then increases, the mass fraction of titanodiopside increases continuously, while the gehlenite content increases first and then decreases. Excessive magnesium oxide promotes the generation of magnesium aluminate spinel [19,27]. The increase in calcium oxide content facilitates perovskite formation and converts anorthite and diopside into akermanite, which further enhances the generation of perovskite [28,29]. Silicon dioxide induces the transformation of titanium-rich phases from perovskite to rutile and simplifies the occurrence state of titanium in slag [29–31].

2.1.2. Break Point Temperature

The break point temperature (T_{Br}) refers to the critical temperature at which the viscosity of slag drops sharply on the viscosity–temperature curve. The temperature corresponding to the tangent point where the viscosity–temperature curve intersects the line with a slope of −1 is the melting temperature, which represents the critical point where the flow state of slag changes abruptly. When the temperature drops below this critical value, slag fluidity deteriorates evidently [32,33].

Titanium dioxide is the main valuable component in titanium-bearing slags, and its content variation exerts a remarkable influence on the Tbr. According to TiO_2 mass fraction, slags are classified into low-titanium slag (TiO_2 < 10 wt%), medium-titanium slag (10 wt% ≤ TiO_2 < 20 wt%) and high-titanium slag (TiO_2 ≥ 20 wt%). For low-titanium slag, the Tbr decreases markedly with increasing TiO_2 content [34–36]. In contrast, when TiO_2 content rises from 20.43 wt% to 21.93 wt%, the T_{Br} of molten slag increases [37,38].

Figure 3 summarizes the influence of TiO_2 content on T_{Br} in various TBFS systems [14,15,39–43]. As illustrated in Figure 3, the T_{Br} of low-titanium slag continuously declines with increasing TiO_2 content, while the T_{Br} of high-titanium slag first rises and then decreases as TiO_2 content increases.

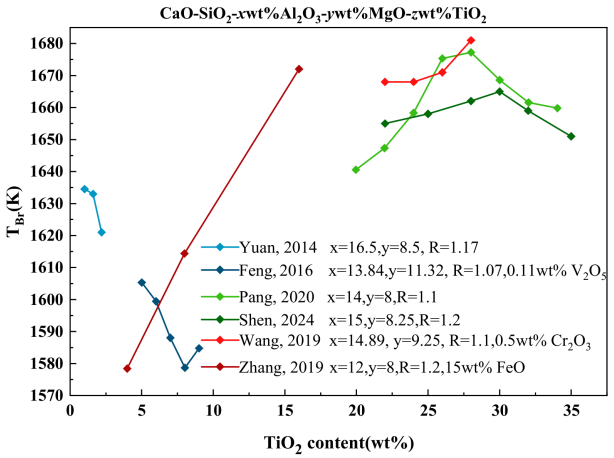


Figure 3. Effect of TiO_2 content on T_{Br} Adapted from Refs. [14,15,39–43].

In high-titanium blast furnace slag, the T_{Br} first rises and then declines with increasing TiO_2 content. When the TiO_2 content is below approximately 30 wt%, high-melting-point compounds such as perovskite are preferentially formed and act as the dominant factor, leading to an increase in T_{Br}. In contrast, when TiO_2 content exceeds 30 wt%, CaO becomes relatively insufficient to sustain continuous perovskite formation. Meanwhile, depolymerization of the silicate network structure and the recovery in the proportion of low-melting-point phases become dominant, resulting in a decrease in T_{Br} [14,41,42].

Increasing contents of Al_2O_3 and MgO both raise the T_{Br} of the slag system. Nevertheless, Al_2O_3 exerts a much stronger promoting effect on slag T_{Br} compared with MgO [36,44]. Figure 4 summarizes the research results on slag T_{Br} from different scholars [24,37,40,45–47]. It can be observed that the T_{Br} of slag increases significantly with rising Al_2O_3 content, whereas the effect of MgO on slag melting characteristics varies among different studies.

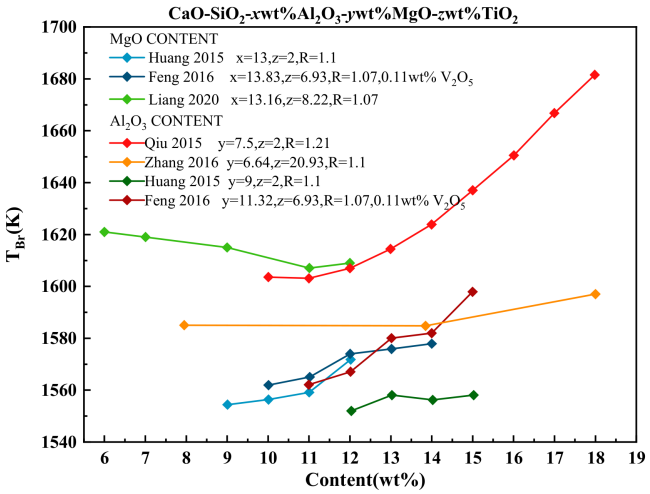


Figure 4. Effect of MgO and Al_2O_3 content on T_{Br} Adapted from Refs. [24,37,40,45–47].

Figure 5 summarizes current research results concerning the effect of slag basicity R2(CaO/SiO_2) on the T_{Br} of TBFS [43,45–50]. It can be seen that the T_{Br} of slag increases significantly with the rise in basicity.

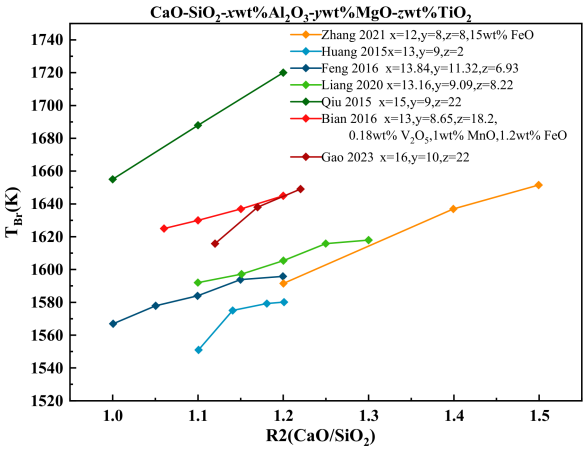


Figure 5. Effect of basicity (CaO/SiO_2) on T_{Br} Adapted from Refs. [43,45–50].

Apart from major components including CaO, MgO and SiO_2, minor oxides such as Cr_2O_3, V_2O_5, MnO and FeO also exert considerable effects on slag melting characteristics [51–54]. Previous studies have demonstrated that increased Cr_2O_3 content in TBFS reacts with MgO and Al_2O_3 to form high-melting-point compounds ($MgCrAlO_4$), thereby raising the T_{Br} [51,54]. Wang [14] reported that the T_{Br} of slag first decreases and then increases with rising Cr_2O_3 content in the slag system. During smelting, partial V_2O_5 and MnO are reduced into molten iron, while the unreduced fraction remains in slag. Generally, V_2O_5 content in slag is less than 0.5 wt%, and MnO content is below 2 wt%. Increasing V_2O_5 content reduces slag T_{Br}, which can be attributed to the formation of low-melting-point calcium vanadate via reaction between V_2O_5 and CaO [52,53]. The T_{Br} continuously declines with increasing MnO content. FeO originates from multiple pathways in slag, including the reduction of Fe_2O_3 and re-oxidation of reduced iron, leading to large variations in FeO content among different slags. As FeO content increases, slag T_{Br} first decreases and then increases. This is because FeO initially reacts with SiO_2 to form low-melting-point fayalite; excessive FeO thereafter enhances the stability of high-melting-point phases and inhibits their decomposition, resulting in elevated T_{Br} [43]. In blast furnace smelting, additives such as CaF_2 (fluorite) and B_2O_3 (from ludwigite) are introduced to improve furnace conditions, which can reduce slag T_{Br} and enhance fluidity.

2.2. Flow Characteristics

Slag fluidity plays a vital role in the smelting process of titanium-bearing slag, which is generally characterized by viscosity. Higher viscosity corresponds to poorer slag fluidity and more difficult slag–iron separation, thus impairing smooth blast furnace operation. By contrast, lower viscosity yields better slag–iron separation performance and higher smelting efficiency. Viscosity testing is generally performed using the RTW integrated melt physical property tester via the rotating cylinder method. A schematic diagram of the equipment is shown in Figure 6.

High-temperature molten blast furnace slag approximates a Newtonian fluid. Relative shear motion between fluid layers generates viscous shear resistance, which conforms to Newton's law of viscosity. The viscosity of molten slag is calculated by measuring the torque acting on the rotating shaft combined with geometric parameters. Standard viscosity oil is used for calibration at room temperature prior to the start of testing.

TiO_2 is an essential constituent of TBFS, mainly originating from iron-bearing raw materials. A small amount of TiO_2 in the blast furnace can protect the furnace lining and extend furnace service life, whereas excessive TiO_2 deteriorates the physicochemical properties of the slag system and exerts adverse impacts on blast furnace smelting. Figure 7 summarizes

the viscosity variation rules of TBFS with different TiO_2 contents [14,15,39,41,42,55–63]. It is observed that slag viscosity decreases and fluidity improves with increasing TiO_2 content.

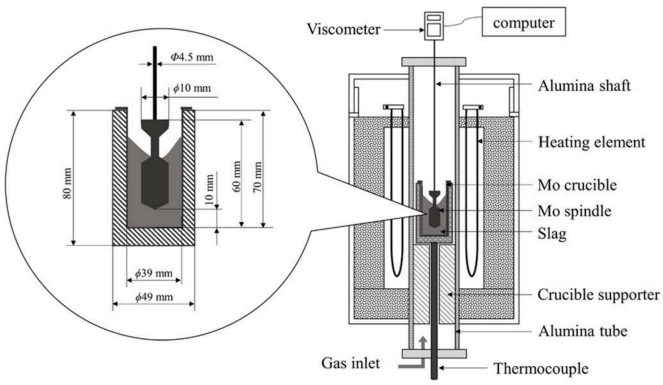


Figure 6. Schematic diagram for the viscosity measurement and dimension of the spindle (Reprinted with permission from Ref. [42]. 2024, Elsevier).

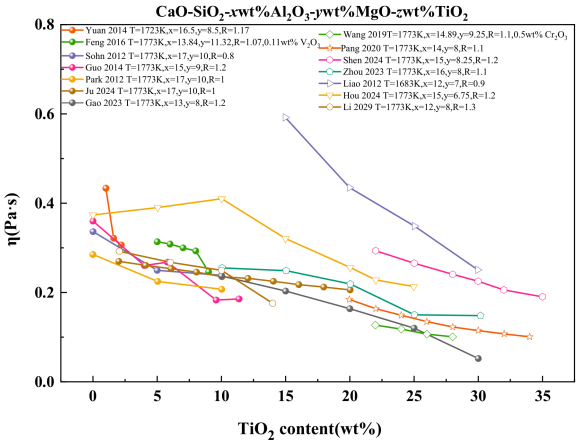


Figure 7. Effect of TiO_2 content on viscosity Adapted from Refs. [14,15,39,41,42,55–63].

Figure 8 summarizes the research results regarding the effects of MgO and Al_2O_3 contents on slag viscosity [24,39,40,45–47,60,62–64]. As shown in the figure, slag viscosity decreases significantly with the increase in MgO content, whereas it rises continuously with the elevation in Al_2O_3 content [40,46].

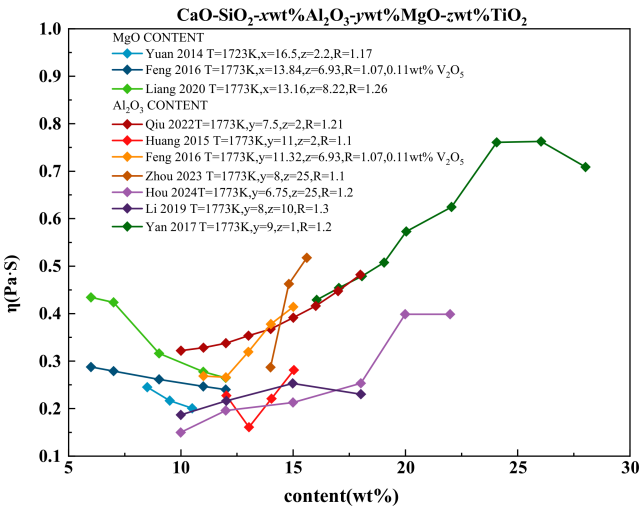


Figure 8. Effect of MgO and Al_2O_3 content on viscosity Adapted from Refs. [24,39,40,45–47,60,62–64].

Figure 9 summarizes the research results on the effect of different basicity values on slag viscosity [45,47–50,55–57,60,62]. As illustrated in the figure, slag viscosity decreases significantly with the continuous increase in basicity [46].

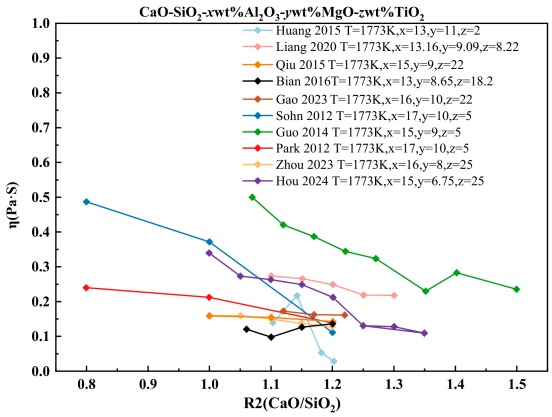


Figure 9. Effect of basicity (CaO/SiO_2) on viscosity Adapted from Refs. [45,47–50,55–57,60,62].

In addition to major components such as CaO, MgO and SiO_2, trace components including Cr_2O_3, V_2O_5, MnO and FeO also exert significant influences on slag flow characteristics. Figure 10 illustrates the effects of different trace components and their contents on slag viscosity [15,48,54,58,65]. It can be observed that with increasing Cr_2O_3 content, slag viscosity decreases when the content is lower than 0.5 wt%, whereas viscosity rises when the content exceeds 0.5 wt%. This is mainly because Cr_2O_3 acts as a network modifier at content $\leq$0.5 wt%, reducing slag polymerization degree and simplifying slag structure, thereby decreasing viscosity. When its content is $\geq$1.5 wt%, refractory solid phases such as perovskite and spinel form, hindering slag flow and resulting in increased viscosity [14]. Slag viscosity declines with the rise in MnO and BaO contents, while it increases with higher CaF_2 content.

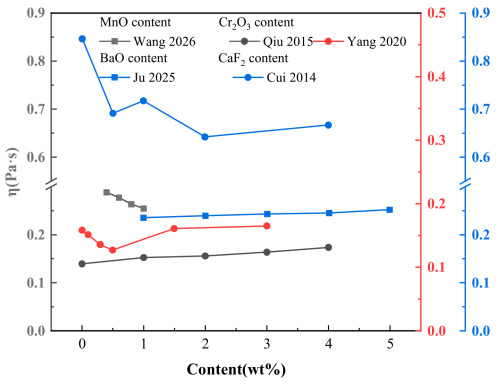


Figure 10. The influence of trace components on the viscosity of slag Adapted from Refs. [15,48,54,58,65].

It can be seen from Figure 6 that increasing TiO_2 content reduces slag viscosity. Nevertheless, the TiO_2 content in furnace burden needs to be controlled in practical blast furnace smelting. This is mainly attributed to the strong reducing atmosphere inside the furnace, where TiO_2 is reduced to low-valence titanium species such as Ti_nO_{2n-1}, TiC and TiN. Notably, TiC and TiN possess melting points above 3000 °C and exist as agglomerated solid particles in molten slag, leading to increased slag viscosity. During blast furnace smelting, TiO_2 undergoes stepwise reduction with the continuous progress of reduction reactions. The content of low-valence titanium oxides and the reduction degree of TiO_2 gradually rise, resulting in continuously increased slag viscosity [66–69]. TiC, TiN and $Ti(C_xN_y)$ can raise

slag T_{Br} and viscosity to varying degrees. Figure 11 shows their effects on slag viscosity, revealing that the viscosity-enhancing effect of titanium carbonitrides follows the order: TiC > $TiC_{0.3}N_{0.7}$ > TiN [67–70].

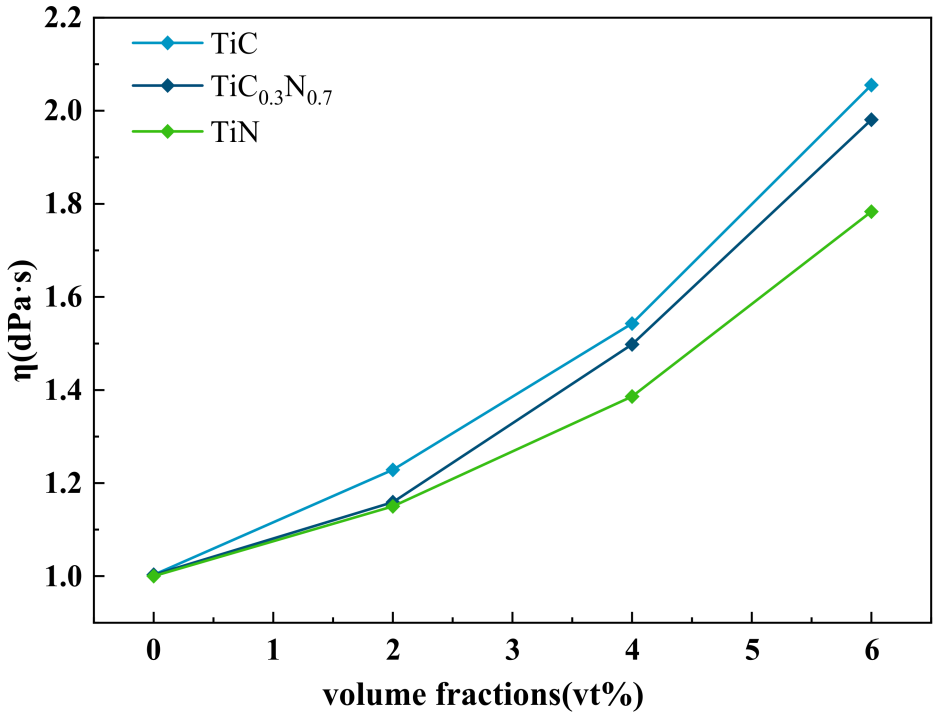


Figure 11. Effects of TiC, TiN and Ti(C_xN_y) with different volume fractions on slag viscosity.

2.3. Analysis of Slag Phase, Structure and Its Influence Mechanism

Variations in slag melting performance and viscous behavior are directly induced by changes in slag phase composition and network microstructure. Both the rising content of high-melting-point phases and the enhanced polymerization degree of slag network can increase slag viscosity and T_{Br}. Therefore, phase analysis and microstructure characterization are indispensable components in the research of slag thermophysical properties. This section reviews recent research findings concerning slag network structure and phase transformation, and clarifies the coupling relationships between slag composition–phase evolution, microstructure–viscosity, and microstructure–melting behaviors.

Variations in the polymerization degree of slag network structure and phase composition are the dominant factors responsible for changes in slag melting and flow characteristics. In the 1930s, Zachariasen [71] proposed the random network theory for oxide glasses, which overturned the traditional microcrystallite hypothesis. Warren et al. [72] subsequently verified the authenticity of this structure through experiments. This theory was gradually introduced into metallurgical molten slag systems, and after continuous improvement by numerous scholars, a theoretical system for the network structure of multicomponent silicate slags was established. Meanwhile, structural parameters including the bridging-oxygen number Q_n of silicon–oxygen tetrahedra and the non-bridging oxygen per tetrahedral cation ratio (NBO/T) were adopted to characterize polymerization degree [73–75]. Taking conventional blast furnace slag as an example, its microscopic structure is built up by silicon–oxygen tetrahedra $[SiO_4]^{4-}$ acting as network formers, which link via bridging oxygen to form chain-like, layered or three-dimensional network structures. Partial aluminum ions enter the network in the form of aluminum–oxygen tetrahedra $[AlO_4]^{5-}$ to construct aluminosilicate composite structures.

Figure 12a presents the phase diagram of the quinary slag system calculated by the thermodynamic software FactSage 6.4 [40]. It can be observed that the investigated slag belongs to low-titanium blast furnace slag and is mainly located in the melilite primary phase region. With all other components kept constant, the liquidus temperature of the slag first decreases and then rises as the TiO_2 content increases. When the TiO_2 content exceeds 8 wt%, the primary phase region transforms into the calcium titanate ($CaTiO_3$) phase region. This is the primary reason why the turning-point temperature rebounds when the TiO_2 content is higher than 8%.

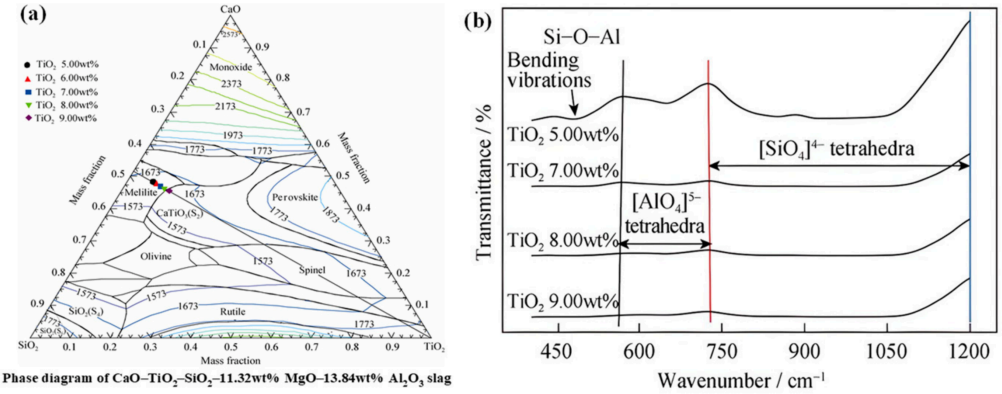


Figure 12. (**a**) Phase diagrams of five-component slag system under different conditions—CaO–TiO_2–SiO_2–11.32 wt% MgO–13.84 wt% Al_2O_3 [40]; (**b**) FTIR spectra of slags with different TiO_2 contents [40]. (Reprinted with permission from Ref. [40]. 2016, Springer Nature).

The FTIR spectra (Figure 12b) reveal that with rising TiO_2 content, the intensities of characteristic vibrational absorption peaks for main structural units including $[SiO_4]^{4-}$, $[AlO_4]^{5-}$, Si–O–Al and Si–O–Al gradually weaken. This indicates that TiO_2 addition causes depolymerization of the network structure in titanium-bearing slag, which macroscopically reduces T_{Br} and viscosity. It is worth noting that although depolymerization of the silicate network occurs, no characteristic Ti–O peaks are observed in the FTIR spectra. The slag systems studied by Wang et al. [14] and Chang et al. [15] contained lower TiO_2 contents, yet their conclusions are basically consistent. Although the overall turning-point temperature rose in the research conducted by Zhang et al. [43]., their experiments adopted relatively large incremental intervals of TiO_2 content (4 wt%, 8 wt% and 16 wt%). Meanwhile, relevant microscopic characterization and mechanism analysis were not performed, so the intrinsic influencing mechanism remains unclear.

Figure 13 shows the Raman test results and NBO/Si values of high-titanium blast furnace slag with different TiO_2 contents. Figure 12 shows that the Raman shift moves toward lower wavenumber (900 cm^{-1} → 790 cm^{-1}). The proportion of Ti–O tetrahedra/octahedra in slag increases gradually, and the slag system transitions from a silicate system to a titanate system. Meanwhile, the content of non-bridging-oxygen bonds in slag increases, indicating that the polymerization degree of the slag network structure decreases, the viscosity of the slag keeps decreasing. By comparing previous studies on titanium-bearing slag structures, it can be found that the viscosity of molten slag decreases gradually with the rising titanium dioxide content when shifting from low-titanium to high-titanium slag systems. This indicates that the evolution of slag microstructure is the dominant factor responsible for the variation in viscosity [14,15,39,41,42,55–63].

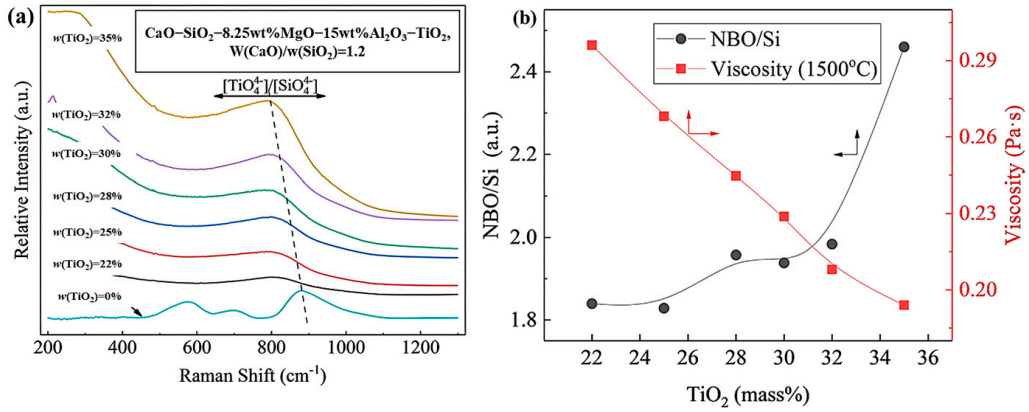


Figure 13. (**a**) Raman spectra of the CaO–SiO_2–MgO–Al_2O_3–TiO_2 slag with different TiO_2 contents; (**b**) effect of TiO_2 content on the value of NBO/Si and the viscosity of slag at 1500 °C [42]. (Reprinted with permission from Ref. [42]. 2024, Elsevier).

By contrast, the proportion of the high-melting-point perovskite phase continuously rises with increasing TiO_2 content. These two factors jointly determine the T_{Br} and viscosity of slag. When the TiO_2 content is below 30 wt%, the increased proportion of the perovskite phase acts as the dominant factor, leading to higher slag T_{Br}. When TiO_2 content exceeds 30 wt%, CaO becomes relatively insufficient, and the decreased polymerization degree of the network structure dominates, resulting in reduced T_{Br} [14,41,42].

Figure 14 presents relevant research results reported by different scholars [40,47]. It can be observed from Figure 14a,c that the major phase regions of the two phase diagrams are essentially identical, with the primary discrepancy lying in the area of the melilite phase region; the melilite phase region in Figure 14a is markedly smaller than that in Figure 14c. This difference mainly originates from the slightly higher TiO_2 content (8.22 wt%) in the slag system investigated in the former study. A larger $CaTiO_3$ primary phase region is formed at the expense of the melilite phase region. The initial research composition (MgO = 6 wt%) falls within the primary crystallization region of $CaTiO_3$. As MgO content rises, the primary crystallization region shifts toward the melilite and spinel phase regions, which causes the T_{Br} to first decrease and then increase. In contrast, the initial composition of the latter study (MgO = 10 wt%) is located inside the melilite phase region. Raising MgO content shifts the primary crystallization region toward the spinel phase region. The elevated MgO concentration facilitates the precipitation of spinel phases, which further brings about a continuous increase in the T_{Br}. For CaO/SiO_2, an increase in basicity raises the content of high-melting-point phases such as perovskite and calcium aluminate in the system, thereby elevating its transition temperature [46,47].

In addition, both CaO and MgO are basic oxides that dissociate into Ca^{2+}, Mg^{2+} and O^{2-}, Ca^{2+}, Mg^{2+} in molten state. Ca^{2+}, Mg^{2+} penetrate into the silicate network structure to stabilize it, whereas the released O^{2-} breaks down the silicate network. As indicated by the FTIR spectra in Figure 14b,d, the intensities of characteristic vibrational absorption peaks for $[SiO_4]^{4-}$, $[AlO_4]^{5-}$ and Si–O–Al and Si–O–Al gradually weaken with rising basicity, demonstrating that the polymerization degrees of silicon–oxygen and aluminum–oxygen networks continuously decrease. Meanwhile, increased basicity promotes the formation of high-melting-point phases such as perovskite and dicalcium silicate, thus significantly raising the T_{Br}. Since viscosity is largely governed by network structure, slag viscosity declines continuously [46,47].

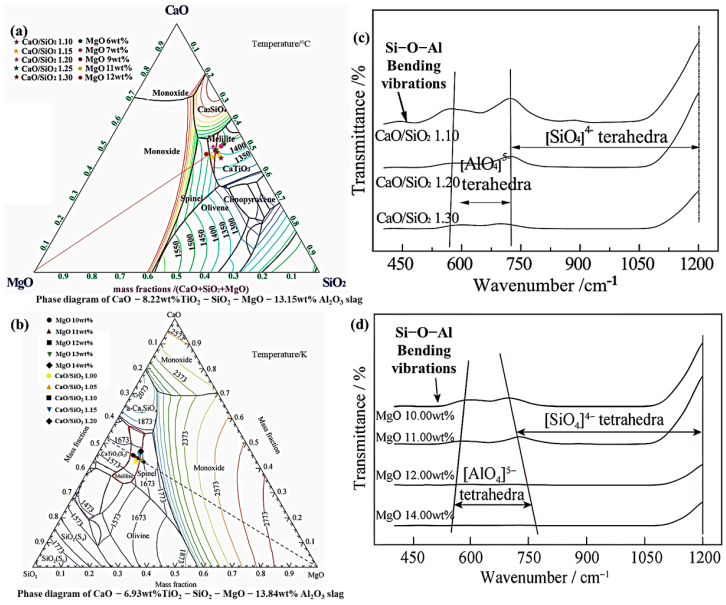


Figure 14. (**a**) Phase diagram of CaO–8.22 wt% TiO_2–SiO_2–MgO–13.15 wt% Al_2O_3 slag [47]; (**b**) FTIR spectra of slags with different basicities [47]; (**c**) phase diagram of CaO–6.93 wt% TiO_2–SiO_2–MgO–13.84 wt% Al_2O_3 slag [40]; (**d**) FTIR spectra of slags with different MgO content [40]. (Reprinted with permission from Ref. [40]. 2016, Springer Nature). (Reprinted with permission from Ref. [47]. 2020, Taylor & Francis).

Figure 15 presents the quinary phase diagram of CaO–8.22 wt %TiO_2–SiO_2–11.32 wt% MgO–Al_2O_3 and FTIR spectra of slags with varying Al_2O_3 contents. It can be seen from the phase diagram that the primary crystallization region shifts toward the spinel phase region with increasing Al_2O_3 content and the liquidus temperature gradually approaches 1673 K. According to XRD test results, the proportion of high-melting-point aluminosilicates rises as Al_2O_3 content increases, which elevates the T_{Br}. In addition, it can be observed from Figure 15b that the characteristic peaks corresponding to the asymmetric stretching vibration of $[AlO_4]^{5-}$ and the bending vibration of Si–O–Al become intensified and the polymerization degree of the slag network increases significantly. This demonstrates that raising alumina content transforms the silicate network into an aluminosilicate network with a higher polymerization degree. Studies have shown that rising Al_2O_3 content significantly increases the content of high-melting-point Mg–Al spinel in slag. Meanwhile, Al^{3+} replaces Si^{4+} to form Si–Al–O complex anions, increasing the polymerization degree of the slag network and thus markedly elevating T_{Br} [24,37,45,46].

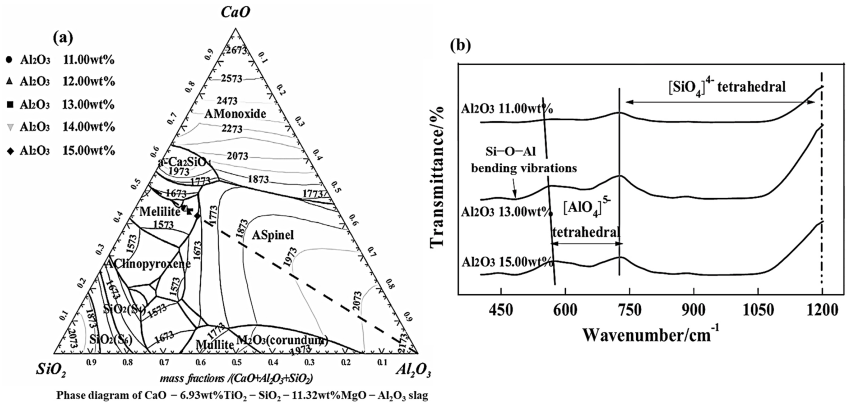


Figure 15. (**a**) Phase diagram of CaO–8.22 wt% TiO_2–SiO_2–11.32 MgO–Al_2O_3 slag [46]; (**b**) FTIR spectra of slags with different Al_2O_3 content [46]. (Reprinted with permission from Ref. [46]. 2016, Wiley).

MnO, as a basic oxide, dissociates free oxygen ions (O^{2-}) that react with bridging oxygen (O°) to depolymerize the silicate network. Second, MnO reacts with Al_2O_3 under specific conditions to form melilite, breaking Al–O tetrahedra and reducing their quantity. The depolymerization effect of MnO is more pronounced at low temperatures, improving slag fluidity [15]. When basicity is low ($\leq$0.9), BaO can substitute for CaO in slag. Dissociated Ba^{2+} disrupts complex silicate anionic structures and decomposes them into simple anions, reducing internal friction among ions. It also decreases molten slag surface tension. These two effects significantly lower slag viscosity and enhance fluidity [58]. When CaF_2 is added, F^- breaks silicate anionic structures and generates low-melting-point cuspidine, while inhibiting the formation of TiC and TiN to reduce slag viscosity. However, charging CaF_2 from the furnace top shifts the soft-melting zone upward; thus, it should be injected through tuyeres. Excessive addition erodes the furnace lining, so its dosage must be strictly controlled [54].

Owing to their high melting points, TiN, TiC and $TiC_{0.3}N_{0.7}$ exist as solid particles and exert negligible effects on slag network structure. They increase viscosity mainly through the volume blocking effect and interfacial adsorption, which amplify their apparent volume and raise flow resistance of the molten slag. As inert particles, TiN adsorbs via size effect and interfacial electronegativity, leading to apparent volume expansion and higher-than-theoretical viscosity enhancement [68]. Unsaturated surface Ti ions of $TiC_{0.3}N_{0.7}$ adsorb molten slag anions and entrap liquid phases, rapidly enlarging its apparent volume, hindering melt sliding and promoting crystallization [70]. With an irregular morphology, TiC strengthens inter-particle interactions. Combined with volume blocking and interfacial adsorption, it forms a three-fold viscosity-enhancing mechanism, exhibiting the strongest thickening effect [67].

3. Conclusions and Prospect

According to existing studies, variations in the melting and flow characteristics s of TBFS are directly governed by changes in slag network structure and phase composition. Increased polymerization degree of the network structure and formation of high-melting-point phases raise slag viscosity and T_{Br}, and vice versa; both are closely associated with variations in slag chemical composition. Based on current research on melting and flow characteristics, the main conclusions are drawn as follows:

(1) Variation law of flow characteristics: O^{2-} ions ionized from basic oxides such as CaO, MgO, BaO and MnO in molten state combine with bridging oxygen (O°), while Ti–O octahedra form from TiO_2 under molten conditions. Both effects disrupt the silicate network structure and reduce polymerization degree, thereby lowering viscosity. By contrast, Al^{3+} ionized from Al_2O_3 replaces Si^{4+} to form Si–Al–O complex anions, increasing the polymerization degree of the slag network. Excessive MgO and Al_2O_3 lead to the formation of Mg-Al spinel, while excessive CaO and TiO_2 produce perovskite, calcium monosilicate and dicalcium silicate. Excess high-melting-point phases cause a sharp rise in viscosity. Under reducing conditions, substances such as TiC and TiN are generated, which significantly deteriorate slag fluidity.

(2) Variation law of melting characteristics: Changes in the content of high-melting-point substances are the primary factor raising T_{Br}. Although increased basicity reduces the polymerization degree of slag structure, the formation of high-melting-point phases including calcium monosilicate and dicalcium silicate dominates, resulting in higher T_{Br}. Increased Al_2O_3 content generates spinel-type high-melting-point phases and raises network polymerization degree, thus elevating T_{Br}. Under an inert atmosphere, TiO_2 greatly reduces network polymerization degree and viscosity. Nevertheless, rising TiO_2 content increases the proportion of perovskite and raises T_{Br}; when TiO_2 content exceeds 30 wt%,

CaO becomes relatively insufficient, leading to decreased T_{Br}. When the MgO content is low, increasing the MgO content reduces the slag T_{Br}; however, when the content is high, high-melting-point spinel phases will form, causing the T_{Br} to rise.

Research on the metallurgical physicochemical properties of titanium slag from vanadium–titanium magnetite blast furnaces possess not only important academic value but also far-reaching practical significance for promoting the sustainable development of the iron–steel and titanium industries. Existing studies have clarified the correlation mechanism of "chemical composition–mineral composition–metallurgical physicochemical properties–smelting indexes" of titanium slag, laying a theoretical foundation for process optimization. However, current slag system studies mainly focus on TiO_2 content below 30 wt% under oxidizing or inert atmospheres. In practical blast furnaces with a strong reducing atmosphere, TiO_2 in slag is reduced to low-valence titanium oxides and Ti(C,N). Therefore, single TiO_2-based research cannot fully reflect the variation rules of physicochemical properties in actual systems. Current thermodynamic and kinetic studies are conducted independently, lacking a unified coupled prediction model for the two fields, which makes it difficult to quantify the effect of Ti(C,N) precipitation on the rheological properties of molten slag under a reducing atmosphere. Further research shall combine high-temperature in situ characterization to clarify the evolution law of composition–phase–structure in ultra-high-titanium slag, and establish a thermodynamics–kinetics coupled mechanism model. The model will be verified based on industrial field data, and process optimization will be carried out focusing on slag basicity, MgO/Al_2O_3 ratio and injection system. Balancing smooth blast furnace operation and titanium resource recovery, this work can provide theoretical support for the efficient industrial smelting of ultra-high-titanium magnetite.

Author Contributions: Conceptualization, S.W., Y.G., L.Y. and F.C.; investigation, G.L., M.C. and J.Z.; resources, Y.G., S.W. and M.C.; data curation, G.L., Y.H., M.C. and J.Z.; writing—original draft preparation, G.L., Y.H., L.Y. and J.Z.; writing—review and editing, S.W., Y.G., F.C., L.Y. and M.C.; supervision, Y.G., S.W., M.C. and L.Y.; project administration, F.C., L.Y., M.C. and J.Z.; funding acquisition, Y.G., S.W., F.C., L.Y. and M.C. All authors have read and agreed to the published version of the manuscript.

Funding: This research was funded by the Collaborative Project of State Key Laboratory of Vanadium and Titanium Resources Comprehensive Utilization "Study on Basic and Applied Technologies for Blast Furnace Smelting of Vanadium-Titanium Magnetite Under Full Pellet Burden Condition" (Grant No. FTGZ2024-02) and National Natural Science Foundation of China (Grant No. 52574394).

Data Availability Statement: No new data were created or analyzed in this study. Data sharing is not applicable to this article.

Conflicts of Interest: Author Mao Chen was employed by the company Pangang Group Research Institute Co., Ltd. The remaining authors declare that the research was conducted in the absence of any commercial or financial relationships that could be construed as a potential conflict of interest.

Nomenclature

R2	Binary basicity, $w(CaO)/w(SiO_2)$
w(x)	Mass fraction of component x, wt%
T_{Br}	Break point temperature,°C
η	Slag viscosity, Pa·s/dPa·s
NBO/T	Ratio of non-bridging oxygen to tetrahedral cations
TBFS	Titanium-bearing blast furnace slag(s)
VTM	Vanadium–titanium magnetite
XRD	X-ray diffraction
FTIR	Fourier transform infrared spectroscopy

References

1. Yang, Y.; Hui, B.; Yan, S.; Chen, C.; Deng, J. Overview of Global Vanadium-titanium Magnetite Resources and Comprehensive Utilization. *Multipurp. Util. Miner. Resour.* **2023**, *44*, 1–11.
2. Zhang, X.; Zeng, Y.; Chen, L.; Song, H.; Ou, Y.; Liu, X. Research status and prospect of comprehensive utilization of blast furnace titanium slag. *Environ. Eng.* **2015**, *33*, 100–104.
3. Zhang, S.; Hu, P.; Rao, J.; Wang, Z.; Zhang, J.; Zong, Y. Current status of comprehensive utilization of vanadium-titanium magnetite and feasibility analysis of HIsmelt smelting. *J. Cent. South Univ. (Nat. Sci. Ed.)* **2021**, *52*, 3085–3092. [CrossRef]
4. Zhang, L.; Wang, C. Research progress on mineral processing technology and comprehensive utilization of vanadium-titanium magnetite resources. *Conserv. Util. Miner. Resour.* **2023**, *43*, 127–137.
5. Gao, Y.; Gui, Y.; Song, C.; Hu, B. Current status and prospect of comprehensive utilization of high-titanium blast furnace slag. *Compr. Util. Miner. Resour.* **2019**, *1*, 6–10.
6. Wang, S.; Guo, Y.; Jiang, T.; Chen, F.; Zheng, F. Current status of comprehensive utilization and industrial development direction of vanadium-titanium magnetite. *China Metall.* **2016**, *26*, 40–44.
7. Bai, C. Study on Several Physicochemical Problems of Titanium-Bearing Blast Furnace Slag. Ph.D. Thesis, Chongqing University, Chongqing, China, 2003.
8. Zhang, X. Research on Metallurgical Properties of Ultra-High Al_2O_3 Blast Furnace Slag in Shigang Iron and Steel. Master's Thesis, Hebei United University, Tangshan, China, 2013.
9. Jing, J.; Guo, Y.; Zheng, F.; Xie, X.; Yang, L.; Chen, F. Research progress on comprehensive utilization of titanium-bearing blast furnace slag. *Met. Mine* **2018**, *4*, 185–191.
10. Lu, P. Research progress and prospect analysis of industrialization for comprehensive utilization of Panzhihua blast furnace slag. *Iron Steel Vanadium Titan.* **2013**, *34*, 33–38. [CrossRef]
11. Chuan-Guan News. Comprehensive Utilization Rate of Panxi Titanium Resources will Increase from 28% to 60%, Panzhihua Iron and Steel Technology Creates High-Value Utilization of High-Titanium Blast Furnace Slag[EB/OL]. Available online: https://cbgc.scol.com.cn/news/4104617 (accessed on 15 April 2026).
12. Xie, H.; Yu, W.; You, Z.; You, Z.; Lv, X.; Bai, C. The Effect of Titanium Carbonitride on the Viscosity of High-Titanium-Type Blast Furnace Slag. *Metals* **2019**, *9*, 395. [CrossRef]
13. Tang, S.; Ding, X.; Dong, Y.; Liu, C. Influence of w(MgO) on Viscous Flow Property of HighTi-containing Blast Furnace Slag. *Chin. J. Mater. Res.* **2016**, *30*, 443–447.
14. Wang, J. Study on Phase Structure and Viscous Flow Properties of Chromium-Containing High-Titanium Blast Furnace Slag. Master's Thesis, Chongqing University, Chongqing, China, 2019.
15. Wang, H.; Ge, Y.; Huang, H.; Meng, Q.; Wang, P.; Long, H. Effect of MnO on metallurgical properties of high-alumina blast furnace slag containing TiO2: Viscosity, structure, and desulfurization capacity. *Ceram. Int.* **2026**, *52*, 2332–2345. [CrossRef]
16. Feng, C.; Chu, M.; Tang, J.; Liu, Z. Main metallurgical properties and phases of different types of titanium-bearing blast furnace slags. *J. Cent. South Univ. (Nat. Sci. Ed.)* **2016**, *47*, 2556–2562.
17. Xu, Y.; Li, D.; Yang, S.; Cai, Y. Research progress on comprehensive utilization of titanium-bearing blast furnace slag. *Compr. Util. Miner. Resour.* **2021**, *1*, 23–31.
18. Li, D. Selective Precipitation and Dissociation of Valuable Components in Blast Furnace Slag. Ph.D. Thesis, Northeastern University, Shenyang, China, 2005.
19. Yang, S.; Feng, Y.; Wang, M.; Liu, Q.; Dong, J.; Chi, Y.; Xiao, Y. Occurrence forms of titanium and calculation of phase crystallization properties in titanium-bearing blast furnace slag. *Iron Steel* **2025**, *60*, 179–189.
20. Shi, Z.; Liu, J. Discussion on phase evolution of high-titanium blast furnace slag before and after selective reduction. *Metall. Anal.* **2017**, *37*, 14–19.
21. Yan, H.; Liu, H.; Chen, B.; Hu, M. Effect of TiO_2 on properties and structure of high-alumina blast furnace slag. *Iron Steel Vanadium Titan.* **2022**, *43*, 118–124.
22. Hu, M.; Wei, R.; Yin, F.; Liu, L.; Deng, Q. Effect of TiO_2 content on the crystallization behavior of titanium-bearing blast furnace slag. *JOM* **2016**, *68*, 2502–2510. [CrossRef]
23. Zhang, Y.; Zhao, Z.; Liu, Z.; Pan, W. Effect of TiO_2 on phase transformation and viscosity of primary titanium-bearing blast furnace slag. *China Metall.* **2019**, *29*, 6–11.
24. Qiu, G.; Miao, D.; Cai, M.; Li, X.; Zhan, D.; Liu, Y. Viscosity and melting properties of titanium-bearing blast furnace slag. *Iron Steel* **2022**, *57*, 42–52. [CrossRef]
25. Deng, M.; Han, X.; Liu, L.; Zhang, D.; Li, Y. Effect of MgO on mineral phase structure and metallurgical properties of medium-titanium blast furnace slag. *Iron Steel* **2016**, *51*, 14–17.
26. Liang, H.; Feng, C.; Chu, M.; Tang, J.; Wang, W. Effect of Al_2O_3 on metallurgical properties of vanadium-titanium blast furnace slag and viscosity prediction model. *J. Cent. South Univ. (Nat. Sci. Ed.)* **2019**, *50*, 514–520.

27. Li, Y.; Sun, C.; Yang, S.; Wang, S.; Zhou, Y.; Zhao, Z.; Si, Z. Effects of TiO_2 and MgO on phase precipitation of titanium-bearing blast furnace slag during cooling. *Mater. Res. Appl.* **2023**, *17*, 1150–1154.
28. Li, Y.; Lou, T.; Sui, Z. Effects of CaO and MnO on perovskite crystallization in titanium-bearing blast furnace slag. *J. Iron Steel Res.* **2000**, *3*, 1–4.
29. Feng, X.; Lai, F.; Li, J.; Liu, Q.; Ren, S.; Yang, J. Crystallization behaviors and properties of Ti-bearing blast furnace slag-based glass ceramics with varying CaO/SiO_2 mass ratio. *J. Aust. Ceram. Soc.* **2022**, *58*, 597–605. [CrossRef]
30. Han, J.; Zhang, J.; Zhang, J.; Chen, X.; Zhang, L.; Tu, G. Combined effect of SiO_2 and O_2 on the crystallization behavior of modified Ti-bearing blast furnace slag. *ACS Omega* **2020**, *5*, 8619–8628. [CrossRef] [PubMed]
31. Li, J. *Fundamental Research on Enrichment and Separation of Titanium in Panzhihua Titanium-Bearing Blast Furnace Slag*; Peking University: Beijing, China, 2012.
32. Wang, X. *Ferrous Metallurgy: Ironmaking Part*; Metallurgical Industry Press: Beijing, China, 2014.
33. Lu, Y.; Yang, G. *Ironmaking Technology*; Metallurgical Industry Press: Beijing, China, 2010.
34. Shi, L.; Li, R.; Long, P.; Xu, X. Effects of Al_2O_3 and TiO_2 contents on viscous flow characteristics and mineral composition of titanium-bearing blast furnace slag. *Shanxi Metall.* **2017**, *5*, 1–3.
35. Wang, Z.; Sun, H.; Zhang, L.; Zhu, Q. Phase equilibria in the TiO_2-rich part of the TiO_2–CaO–SiO_2–10 wt% Al_2O_3 system at 1773 K and 1873 K. *J. Alloys Compd.* **2016**, *671*, 137–143. [CrossRef]
36. Zhang, J.; Shi, L.; Ao, W. Melting property of high-alumina low-titanium blast furnace slag. *J. Iron Steel Res.* **2010**, *22*, 16–19.
37. Zhang, S.; Xu, Y.; Xie, J.; Hu, J. Effects of main components of blast furnace slag on its melting characteristics and viscosity. *Nonferrous Met. Eng.* **2016**, *6*, 50–54.
38. Ye, D. *Practical Handbook of Inorganic Thermodynamic Data*; Metallurgical Industry Press: Beijing, China, 1981.
39. Yuan, X.; Zhang, J.; Mao, R.; Liu, Z.; Zhu, G. Viscosity and melting properties of low-titanium blast furnace slag. *Chin. J. Process Eng.* **2014**, *14*, 664–670.
40. Feng, C.; Chu, M.; Tang, J.; Qin, J.; Li, F.; Liu, Z. Effects of MgO and TiO_2 on the viscous behaviors and phase compositions of titanium-bearing slag. *Int. J. Miner. Metall. Mater.* **2016**, *23*, 868–880. [CrossRef]
41. Pang, Z.; Lv, X.; Jiang, Y.; Ling, J.; Yan, Z. Blast furnace ironmaking process with super-high TiO_2 in the slag: Viscosity and melting properties of the slag. *Metall. Mater. Trans. B* **2020**, *51*, 722–731. [CrossRef]
42. Shen, F.; Zhang, G.; Tian, J.; Zheng, H.; Gao, Q.; Jiang, X. Effect of TiO_2 on the structural properties and viscosity of CaO–SiO_2–8.25%MgO–15%Al_2O_3–TiO_2 slags. *J. Non-Cryst. Solids* **2024**, *640*, 123114. [CrossRef]
43. Zhang, Y.; Wang, D.; Chen, S.; Liu, Z.; Pan, W.; Zhao, Z. Effects of basicity, FeO, and TiO_2 on phase transformation and viscosity of TiO_2 bearing primary slag in blast furnace. In *Characterization of Minerals, Metals, and Materials 2021*; Springer: Cham, Switzerland, 2021; pp. 187–199.
44. Xie, H.; Qin, X.; Zheng, K.; Jiang, S. Analysis of influencing factors on melting temperature of high-titanium blast furnace slag. *China Metall.* **2017**, *27*, 13–19.
45. Huang, H.; Lv, Q.; Cao, L.; Liu, X.; Zou, Y.; Ding, H. Fluidity of low-titanium blast furnace slag. *Iron Steel Vanadium Titan.* **2015**, *36*, 78–83.
46. Feng, C.; Chu, M.; Tang, J.; Tang, Y.; Liu, Z. Effect of CaO/SiO_2 and Al_2O_3 on viscous behaviors of the titanium-bearing blast furnace slag. *Steel Res. Int.* **2016**, *87*, 1274–1283. [CrossRef]
47. Liang, H.; Chu, M.; Feng, C.; Tang, J.; Liu, Z.; Wang, W. Optimisation study and affecting mechanism of CaO/SiO_2 and MgO on viscous behaviours of titanium-bearing blast furnace slag. *Ironmak. Steelmak.* **2020**, *47*, 106–117.
48. Qiu, G.; Chen, L.; Zhu, J.; Lv, X.; Bai, C. Effect of Cr_2O_3 addition on viscosity and structure of Ti-bearing blast furnace slag. *ISIJ Int.* **2015**, *55*, 1367–1376. [CrossRef]
49. Bian, L.; Gao, Y. Influence of B_2O_3 and basicity on viscosity and structure of medium titanium bearing blast furnace slag. *J. Chem.* **2016**, *2016*, 6754593. [CrossRef]
50. Gao, H.; Tang, J.; Chu, M.; Zhong, S.; Liu, Z. Effects of MgO/Al_2O_3 and CaO/SiO_2 ratios on viscosity of high titanium-bearing blast furnace slag. *J. Iron Steel Res. Int.* **2023**, *30*, 456–464. [CrossRef]
51. Zhu, J. Study on Flow Properties and Phase Transformation Law of Chromium-Containing High-Titanium Blast Furnace Slag. Master's Thesis, Chongqing University, Chongqing, China, 2014.
52. Lv, Q.; Tang, Q.; Sun, Y. Relationship between slag properties and vanadium oxide reduction in blast furnace smelting of vanadium-titanium magnetite. *Iron Steel Vanadium Titan.* **2016**, *37*, 1–4.
53. Chu, M.; Feng, C.; Tang, J.; Liu, Z. Study on blast furnace slag system of vanadium-titanium magnetite under neutral atmosphere. *J. Northeast. Univ. (Nat. Sci. Ed.)* **2015**, *36*, 1283–1287.
54. Cui, S.; Lv, Q.; Feng, S.; Sun, Y.; Chen, S.; Li, F.; Wan, X.; Kang, Z. Effect of additives on viscosity of titanium-bearing blast furnace slag. *Iron Steel Vanadium Titan.* **2014**, *35*, 68–72.
55. Sohn, I.; Wang, W.; Matsuura, H.; TSUKIHASHI, F.; Min, D. Influence of TiO_2 on the viscous behavior of calcium silicate melts containing 17 mass % Al_2O_3 and 10 mass % MgO. *ISIJ Int.* **2012**, *52*, 158–160. [CrossRef]

56. Guo, D.; Zhang, J.; Lu, D.; Bai, C.; Liu, X. Effect of basicity on viscosity of CaO–SiO_2–Al_2O_3–MgO–TiO_2 slag system. *Iron Steel* **2014**, *49*, 13–17.
57. Park, H.; Park, J.; Kim, G.; Sohn, I. Effect of TiO_2 on the viscosity and slag structure in blast furnace type slags. *Steel Res. Int.* **2012**, *83*, 150–156. [CrossRef]
58. Ju, J.; Li, X.; Wei, L.; Xing, X. Effect of TiO_2 and BaO on viscosity and potassium removal capacity of blast furnace slag. *J. Iron Steel Res. Int.* **2024**, *31*, 2675–2683. [CrossRef]
59. Gao, Y.J.; Liu, R.; Wang, Y.; Liu, Y.; Chen, S.; Deng, Y.; Yu, Q. Viscosity of CaO–SiO_2–Al_2O_3–MgO–TiO_2–FeO slag in HIsmelt process: Influence of TiO_2 content on viscosity and crystallization. *Metall. Mater. Trans. B* **2023**, *54*, 3288–3298. [CrossRef]
60. Zhou, W.; Li, T.; Lan, D.; Sun, C.; Yang, S. Influence of TiO_2, Al_2O_3, and basicity on viscosity and structure of high titanium-bearing blast furnace slag. *Materials* **2023**, *16*, 2575. [CrossRef] [PubMed]
61. Liao, J.; Li, J.; Wang, X.; Zhang, Z. Influence of TiO_2 and basicity on viscosity of Ti-bearing slag. *Ironmak. Steelmak.* **2012**, *39*, 133–139. [CrossRef]
62. Hou, X.; Zhang, B.; Zhang, S.; Zheng, H.; Jiang, X.; Gao, Q.; Shen, F. Effects of slag composition on structure and viscosity of titanium-bearing high-alumina blast furnace slag. *J. Mater. Metall.* **2024**, *23*, 465–471.
63. Li, T.; Sun, C.; Song, S.; Wang, Q. Influences of Al_2O_3 and TiO_2 content on viscosity and structure of CaO–8%MgO–Al_2O_3–SiO_2–TiO_2–5%FeO blast furnace primary slag. *Metals* **2019**, *9*, 743. [CrossRef]
64. Yan, Z.; Lv, X.; Liang, D.; Zhang, J.; Bai, C. Transition of blast furnace slag from silicates-based to aluminates-based: Viscosity. *Metall. Mater. Trans. B* **2017**, *48*, 1092–1099. [CrossRef]
65. Yang, D.; Zhang, F.; Wang, J.; Yan, Z.; Pei, G.; Qiu, G.; Lv, X. Effect of Cr_2O_3 content on viscosity and phase structure of chromium-containing high-titanium blast furnace slag. *J. Mater. Res. Technol.* **2020**, *9*, 14673–14681. [CrossRef]
66. Wan, X.; Pei, H.; Bai, C.; Zhou, P. Reduction of titanium oxides and thickening of titanium slag. *J. Chongqing Univ. (Nat. Sci. Ed.)* **2000**, *5*, 36–39.
67. Zhen, Y.; Zhang, G.; Chou, K. Viscosity of CaO–MgO–Al_2O_3–SiO_2–TiO_2 melts containing TiC particles. *Metall. Mater. Trans. B* **2015**, *46*, 155–161.
68. Zhen, Y.; Zhang, G.; Chou, K.; Mill, K. Influence of TiN on viscosity of CaO–MgO–Al_2O_3–SiO_2–(TiN) suspension system. *Can. Metall. Q.* **2015**, *54*, 340–348. [CrossRef]
69. Lv, Q.; Huang, H.; Chen, S.; Liu, X.; Sun, Y.; Ding, H. Effects of solid carbon and TiC content on properties of titanium-bearing blast furnace slag. *Iron Steel Vanadium Titan.* **2015**, *36*, 84–88.
70. Chen, M.; Chen, B.; Jiang, Y.; Zheng, K.; Hu, M.; Qiu, G. Study of Ti(C,N) formations in TiO_2-containing slags. *Metall. Mater. Trans. B* **2025**, *56*, 1018–1028.
71. Zachariasen, W.H. The atomic arrangement in glass. *J. Am. Chem. Soc.* **1932**, *54*, 3841–3851. [CrossRef]
72. Warren, B.E. X-ray diffraction study of the structure of glass. *Chem. Rev.* **1940**, *26*, 237–255. [CrossRef]
73. Masson, C.R.; Smith, I.B.; Whiteway, S.G. Activities and ionic distributions in liquid silicates: Application of polymer theory. *Can. J. Chem.* **1970**, *48*, 1456–1464. [CrossRef]
74. Mills, K.C. The influence of structure on the physico-chemical properties of slags. *ISIJ Int.* **1993**, *33*, 148–155. [CrossRef]
75. Gaskell, D.R. The thermodynamic properties of the masson polymerization models of liquid silicates. *Metall. Trans.* **1973**, *4*, 185–192. [CrossRef]

Disclaimer/Publisher's Note: The statements, opinions and data contained in all publications are solely those of the individual author(s) and contributor(s) and not of MDPI and/or the editor(s). MDPI and/or the editor(s) disclaim responsibility for any injury to people or property resulting from any ideas, methods, instructions or products referred to in the content.